

A biodiversity-inspired approach to aquatic ecosystem modeling

Jorn Bruggeman¹ and Sebastiaan A. L. M. Kooijman

Vrije Universiteit, Faculty of Earth & Life Sciences, Department of Theoretical Biology, de Boelelaan 1085, 1081 HV Amsterdam, The Netherlands

Abstract

Current aquatic ecosystem models accommodate increasing amounts of physiological detail, but marginalize the role of biodiversity by aggregating multitudes of different species. We propose that at present, understanding of aquatic ecosystems is likely to benefit more from improved descriptions of biodiversity and succession than from incorporation of more realistic physiology. To illustrate how biodiversity can be accounted for, we define the system of infinite diversity (SID), which characterizes ecosystems in the spirit of complex adaptive systems theory as single units adapting to environmental pressure. The SID describes an ecosystem with one generic population model and continuity in species-characterizing parameters, and acquires rich dynamics by modeling succession as evolution of the parameter value distribution. This is illustrated by a four-parameter phytoplankton model that minimizes physiological detail, but includes a sophisticated representation of community diversity and interspecific differences. This model captures several well-known aquatic ecosystem features, including formation of a deep chlorophyll maximum and nutrient-driven seasonal succession. As such, it integrates theories on changes in species composition in both time and space. We argue that despite a lack of physiological detail, SIDs may ultimately prove a valuable tool for further qualitative and quantitative understanding of ecosystems.

Biodiversity poses a perennial problem for ecosystem modelers. Confronted with a reality fraught with species, dependencies, and physiological detail, one cannot help but think that simple models cannot do it justice (Anderson 2005). Simple models aggregate large numbers of species into single state variables, and by doing so they lose the ability to reproduce ranges of behavior shown by detailed species-explicit models (Raick et al. 2006). Also, the use of aggregation puts models at a greater distance from empirical results, first because assimilation of empirically determined, species-specific parameter values to parameters of virtual aggregates of species is a difficult and largely subjective process; second because aggregate models provide only indirect information about individual species observed in the field. Not surprisingly, large ecosystem models that describe many classes of species explicitly have recently gained in popularity (Baretta et al. 1995; Quéré et al. 2005). However, continued diversification of functional groups may create more problems than it solves. Increasing the number of groups within ecosystem models dilutes the available empirical information per model unit, and therefore increases the uncertainty per parameter. Considering the substantial uncertainty already associated with parameters of moderate-size ecosystem models, this route seems unappealing. Also, it is easy to overlook that as the number of variables within an ecosystem model increases, so does the amount of information needed to initialize the model. A utopian species-complete model would require initial abundances of every single ecosystem species (and

their substrates) to arrive at accurate predictions. Even if it were possible, complete retrieval of this information is certain to prove so costly in practice that the actual value of such detailed models for most applications is debatable.

The merits of incorporating more species in ecosystem models are well recognized, but perpetually adding more *explicitly* modeled species primarily brings uncertainty and complexity. Instead, we propose a hybrid approach that builds on simple aggregate models, and bridges voids (in quantitative knowledge) between species classes according to unifying biological principles, e.g., thermodynamic constraints and body size scaling relations. The use of a limited number of functional groups, in combination with interpolation on the basis of unifying principles, replaces the unfeasible amount of species-specific information otherwise needed to model realistic diversity. To allow for interpolation between species, all species are modeled with the same, *omnipotent population model*; interspecific differences are captured by differences in values of key parameters—traits—rather than differences in model structure. Application of unified models to several similar species is not rare (Ebenhöh et al. 1997), but to our knowledge, such unification has not been applied consistently across ecosystems. Indeed, because of the large diversity within such systems, this is not a trivial affair. It places serious demands on the modularity and consistency of the model, and necessitates a modeling approach that spans species and functional groups. Such an approach is the dynamic energy budget (DEB) theory (Kooijman 2000), which has been successful at describing a wide variety of species, and is demonstrably capable of combining traditionally distinct strategies as autotrophy and heterotrophy (Kooijman et al. 2002; Troost et al. 2005).

As a next step toward simple biodiversity-based models, we assume *continuity in trait values*. Traits can take any value, and any combination of different trait values is

¹ Corresponding author (jorn.bruggeman@falw.vu.nl).

Acknowledgments

We thank Bob Kooi and two anonymous reviewers for their comments.

This research was supported by the Netherlands Organisation for Scientific Research (NWO) through grant 635.100.009.

possible in multitrait models. In a sense, we allow for every conceivable hybrid between species. This concept offers a powerful means of system simplification, as illustrated by its application in earlier aquatic ecosystem models (Wirtz and Eckhardt 1996). Continuity in trait space implies that in a model that distinguishes n traits, the state of the system is described by an n -variable probability distribution, its value at any trait coordinate indicating the probability of finding a species with that specific trait value combination. Changes in ecosystem and community structure are captured by the dynamics of the trait value distribution. We distinguish three mechanisms through which these dynamics arise: (1) succession, i.e., differential growth and decay of populations of the various species; (2) physiological adaptation, i.e., changes in the trait value of individuals (e.g., photoacclimation in the classic sense); and (3) genetic evolution, i.e., mutation and selection causing changes in the phenotype (trait values). Succession manifests as the rise of parts of the trait distribution at the expense of other parts, whereas physiological adaptation and evolution cause shifts in the distribution toward (local) fitness optima, on short and long timescales respectively. Each mechanism can be incorporated in trait distribution dynamics (Abrams et al. 1993; Dieckmann and Law 1996; Jiang et al. 2005); in this study we focus exclusively on succession. The resulting approach bears strong resemblance to complex adaptive systems theory (Levin 1998; Leibold and Norberg 2004; Norberg 2004), which aspires to understand (eco)system dynamics in terms of diversity and selection. Independent of the underlying mechanism, the direction and the rate of changes in the trait value distribution are in part governed by trade-offs associated with changes in trait value (Norberg 2004): The combination of (environment-dependent) costs and benefits of traits directs and bounds the evolution of the trait value distribution. Examples of trade-offs in aquatic systems abound. For phytoplankton, increased resource harvesting or defense against predation comes at the expense of growth (Wirtz and Eckhardt 1996), and harvesting of one nutrient comes at the expense of harvesting another (Tilman et al. 1982; Huisman and Weissing 2001).

Where the behavior of traditional ecosystem models is for a significant part determined by parameter values, evolution of the trait value distribution depends on the shape of the initial distribution. If the system is opened to migration, this dependency is reduced as control shifts to the trait distribution of immigrating species. There are sound indications that in aquatic ecosystems migration can play a major role: “[we conceive] the pelagic as an open system where communities are continually reshaped by species immigration” (Cloern and Dufford 2005). With this in mind, we propose to model the ecosystem as a system that continuously experiences immigration of trace quantities of every possible species. Sources of immigrating individuals are not resolved explicitly, but may be found in (1) spatial subsidies (Polis et al. 1997), i.e., immigration from neighboring environments as featured in metapopulation theory (Hanski 1999; Leibold and Norberg 2004); or (2) permanent background concentrations of dormant life stages (e.g., spores, eggs) capable of waking in viable

environments (Anderson and Rengefors 2006). The rate of immigration may vary in time and place, and could—in particular when linked to spatial heterogeneity—correlate with water transports or (turbulent) diffusion, or both. The fate of immigrating species is uncertain. The majority will perish (local extinction), but small subsets of species will at times find a niche, outcompete existing species, and cause the trait distribution to change. The net result is reminiscent of a century-old concept from microbiology: “Everything is everywhere; the environment selects.” (Beijerinck 1913; Baas-Becking 1934).

Summarizing, our approach encompasses three components: (1) an omnipotent population model, (2) trait distributions that capture biodiversity, and (3) continuous immigration of trace quantities of all species. We will refer to systems that incorporate these components as systems of infinite diversity (SIDs). In this study, we demonstrate that a minimal, four-parameter SID for phytoplankton, placed in a detailed one-dimensional setting, reproduces a number of well-known aquatic ecosystem features, including (1) seasonal development of a subsurface chlorophyll maximum independent of a biomass maximum (Fennel and Boss 2003) due to the emergence of a “shade flora” (Sournia 1982*b*; Venrick 1982); (2) seasonal succession linked to variation in nutrient affinity, as proposed by Margalef’s Mandala (Margalef 1978); and (3) the suggestion of trade-offs between harvesting capacities for different resources in random samples of phytoplankton species (Huisman and Weissing 2001). The present incarnation of SIDs proves computationally expensive; in conclusion, however, we discuss recent techniques (Wirtz and Eckhardt 1996; Norberg et al. 2001) that are capable of rendering reasonably accurate, highly efficient parameterizations of SIDs.

Methods

In aquatic ecosystems, biodiversity has historically been extensively studied in terms of phytoplankton competition and succession (Margalef 1978; Tilman 1982; Sommer 1985); to this day, many ecosystem models still aim primarily to resolve and explain the rise and fall of phytoplankton species (Merico et al. 2004; Lancelot et al. 2005). Because of the substantial amount of data and theory available on phytoplankton succession, it presents an ideal test case for the SID approach. We therefore construct a simple model system that is limited to a phytoplankton community and one type of nutrient. The plankton model is loosely based on concepts from DEB theory (Kooijman 2000) and qualitatively resembles previous approaches (Huisman and Weissing 1995; Diehl 2002). Species interaction is implemented as competition for a shared external nutrient pool. The behavior of the model is first evaluated in a nonspatial setting subject to a realistically fluctuating light intensity. Subsequently, we partially resolve the spatial structure of the environment with a water column model; this model incorporates a realistic time- and depth-varying mixing intensity, and resolves the decrease in light intensity with depth.

A model of the phytoplankton community—Phytoplankton species differ quantitatively in numerous features, among which are cell size, resource harvesting ability, and edibility. In environments that are not predation-dominated (e.g., oligotrophic open ocean sites), a good predictor of the competitive ability of individual species is their affinity for nutrients and light (Tilman 1982; Passarge et al. 2006). To account for interspecific differences in nutrient and light affinity, we propose to partition the total biomass of a phytoplankton population into three types: (1) biomass dedicated to light harvesting, (2) biomass dedicated to nutrient harvesting, and (3) structural biomass responsible for growth (cf. Shuter 1979; Geider et al. 1996; Klausmeier et al. 2004). Light-harvesting biomass represents chlorophyll as well as closely associated cellular machinery. Similar to the work of Geider et al. (1996, 1998), we assume a fixed fraction of light-harvesting biomass to consist of chlorophyll, implying that this type of biomass can serve as chlorophyll proxy. Nutrient-harvesting biomass includes compounds directly affecting nutrient consumption (e.g., membrane-bound transporters), as well as any co-occurring machinery. If one accepts that the capacity for nutrient uptake is determined by the surface area of the cell (Munk and Riley 1952; Sournia 1982a), nutrient-harvesting biomass must comprise the “shell” of the cell, i.e., the cell wall and membrane as well as transporters. Then the ratio of nutrient-harvesting biomass to structural biomass can serve as proxy for the surface-to-volume ratio, and for isomorphic species its reciprocal can be a proxy for cell size (Kooijman 2000). However, this relation is obfuscated if diffusion limits nutrient availability (Chisholm 1992), as may occur in oligotrophic environments; we therefore do not explore the link between nutrient-harvesting biomass and size further in this study. Structural biomass represents all biomass that does not contribute to assimilation, but is required to build a living alga; it can be regarded as a measure of population size. In the model we quantify the species-specific distribution of biomass over the three pools by two partition coefficients: m_L represents the quantity of light-harvesting biomass per unit of structural biomass, and m_N represents the quantity of nutrient harvesting biomass per unit of structural biomass. One can interpret these coefficients as harvesting investments: They quantify a species’ investment in resource harvesting, relative to its investment in pure growth. The combination of the partition coefficients and the amount of structural biomass, denoted by V , specifies the amount of light- and nutrient-harvesting biomass: $m_L V$ and $m_N V$, respectively.

A phytoplankton population is assumed to require light and some nutrient (e.g., nitrate) to produce new biomass. The rate of biomass production is governed by the synthesizing unit (SU) expression for colimitation, which offers a flux-based description of classic multisubstrate enzyme kinetics under the assumption of negligible substrate dissociation (Kooijman 1998, 2000; Kuyper et al. 2004). The SU-governed rate at which new biomass is produced equals

$$J_A = \frac{1}{J_{Am}^{-1} + \left(\frac{J_L}{y_L}\right)^{-1} + \left(\frac{J_N}{y_N}\right)^{-1} - \left(\frac{J_L}{y_L} + \frac{J_N}{y_N}\right)^{-1}}$$

in which J_{Am} denotes the maximum rate of biomass production, J_L and J_N the rates at which light and nutrient become available to growth machinery, and y_L and y_N the amounts of light and nutrient needed to produce one unit of biomass. The maximum rate of biomass production is taken proportional to the population size, quantified by the amount of structural biomass: $J_{Am} = r_{max} V$ in which r_{max} denotes the maximum structure-specific rate of biomass production. The internal availabilities of light and nutrient are taken proportional to the external light intensity X_L and nutrient concentration X_N , respectively, and to the amounts of corresponding harvesting biomasses, i.e., $J_L \propto m_L V X_L$ and $J_N \propto m_N V X_N$. The rate at which new biomass is produced can now be written as

$$J_A = \frac{r_{max} V}{1 + \left(m_L \frac{X_L}{K_L}\right)^{-1} + \left(m_N \frac{X_N}{K_N}\right)^{-1} - \left(m_L \frac{X_L}{K_L} + m_N \frac{X_N}{K_N}\right)^{-1}} \quad (1)$$

in which K_L denotes the half-saturation light intensity at $m_L = 1$ and K_N denotes the nutrient half-saturation concentration at $m_N = 1$. The half-saturation coefficients are compound parameters that contain yields y_L and y_N as well as the maximum growth rate r_{max} . Newly produced biomass is distributed over the three biomass pools as specified by the partition coefficients m_L and m_N ; thus, structural biomass is formed at rate

$$J_{VA} = \frac{J_A}{1 + m_L + m_N} \quad (2)$$

We assume that all biomass requires maintenance, i.e., a certain amount of energy per unit time necessary to maintain the cell (Kooijman 2000). Energy for maintenance is obtained through breakdown of organic compounds; mass remineralized in this process re-enters the external nutrient pool. As initial approximation, we will assume that all three biomass types are subject to equal maintenance requirements. Additionally, we assume that only structural biomass can serve as energy source for maintenance; energy stored in harvesting biomasses (e.g., chlorophyll) cannot be regained. Harvesting biomasses simply decay passively along with structural biomass. The rate of structural biomass turnover related to maintenance is now given by

$$J_{VM} = (1 + m_L + m_N) V k \quad (3)$$

in which k denotes the amount of structural biomass required to maintain one unit of (structural or harvesting) biomass per unit time.

The net growth of structural biomass equals the difference between assimilation and maintenance, i.e.

$$\frac{dV}{dt} = J_{VA} - J_{VM} \quad (4)$$

Since the partition coefficients are constant for a given species, this immediately specifies the change in harvesting biomass. The dynamics of light-harvesting and nutrient-harvesting biomass equal $m_L dV / dt$ and $m_N dV / dt$, respectively. We choose to measure phytoplankton biomass

in nutrient units (i.e., $\mu\text{mol nutrient L}^{-1}$), which implies that dynamics of the external nutrient pool mirror the dynamics of the total biomass: For a given change in structural biomass dV/dt , the corresponding change in nutrient equals $-(1 + m_L + m_N)dV/dt$.

The phytoplankton population model serves as basis of a SID in which all differences between phytoplankton species are quantified by differences in harvesting investments m_L and m_N . These traits affect all parts of the metabolism. They enhance resource availability (Eq. 1), but increase the cost for growth (Eq. 2) and maintenance (Eq. 3). This creates a trade-off between harvesting and net growth: If harvesting investments tend to zero, biomass growth stops while (structure-specific) turnover continues, resulting in extinction of the population. If harvesting investments become very high, assimilation saturates, whereas (harvesting-specific) turnover increases linearly, also resulting in extinction. The trait values are thus restricted to a viable region, its environment-dependent contour defined by the trait value combinations for which $dV/dt = 0$. The largest viable region is obtained if light and nutrient availability are infinite; then we obtain the boundary

$$m_L + m_N < -1 + \sqrt{\frac{r_{\max}}{k}}$$

which in combination with the obvious boundaries $m_L > 0$ and $m_N > 0$ renders a triangular viable region. Species outside this region can never achieve a positive growth rate. Initial simulations show that of all species within the viable region, only a small fraction (<20 %) with low trait values attains nonnegligible biomass levels in practice. For all subsequent simulations, we therefore discretize the trait distribution for this smaller region only on a square 25×25 trait value grid; this renders a system composed of 625 virtual phytoplankton species. The dynamics of individual species are governed by Eq. 4, different for each species through the dependency on (species-specific) m_L and m_N . All species share the external nutrient pool, the dynamics of which can therefore be written as sum of contributions of all species i , i.e.,

$$\frac{dX_N}{dt} = - \sum_i (1 + m_{L,i} + m_{N,i}) \frac{dV}{dt} \Bigg|_{\substack{V = V_i \\ m_L = m_{L,i} \\ m_N = m_{N,i}}} \quad (5)$$

Environmental conditions—The structure of phytoplankton communities is often strongly time and space dependent. Seasonal fluctuations in solar radiation and mixing intensity drive succession, most prominently through the initialization of phytoplankton growth in spring (following stratification and increased solar radiation) and its termination in the fall (following increased mixing and decreased radiation). Resource gradients in space—notably the decrease of light intensity with depth—cause the community structure to be strongly space dependent. Generally, one cannot separate the structure and diversity of communities from the heterogeneity of their environment. Biodiversity in nature is sustained at

least partially because of spatiotemporal heterogeneity (Tilman 1982; Tilman et al. 1982; Tilman and Kareiva 1997). Therefore, we study the behavior of the phytoplankton SID in a setting that includes variation in time and space. First, we simulate the phytoplankton community at an open ocean site over 3 yr with a realistic time-varying light intensity, averaged over the top 150 m that constitutes the euphotic zone. Second, we explicitly resolve the vertical structure of the top 400 m of the site with a 100-layer model of the turbulent water column (Burchard et al. 1999; Burchard et al. 2006); this model incorporates an exponential decay of light with depth, and calculates a time- and depth-varying mixing intensity (turbulent diffusivity) from observed weather conditions. The mixing regime controls the distribution of plankton and nutrient over the water column, and thus indirectly affects light and nutrient availability. The physical model used to calculate the surface light intensity and the turbulent diffusivity is described in more detail in Web Appendix 1 (http://www.aslo.org/lo/toc/vol_52/issue_4/1533a1.pdf).

Table 1 lists parameter values and the initial state used for the biological model. The water column is initialized with a nutrient concentration of $4 \mu\text{mol L}^{-1}$, which is the average nitrate concentration across the top 400 m of the simulated open ocean site (Steinberg et al. 2001). An initial structural biomass concentration of $0.5 \mu\text{mol L}^{-1}$ is distributed uniformly over the trait distribution grid, resulting in trace concentrations (0.8 nmol L^{-1}) of each of the 625 possible species. In both setups we open the simulated nutrient–phytoplankton system by imposing a flow through the system. The flow introduces new nutrient and species at concentrations that are taken equal to the above initial levels, and simultaneously exports a fraction of the existing system. In the depth-averaged setup, the flow rate is constant (0.16 d^{-1}), whereas in the spatial setup this rate scales with the turbulent diffusivity, and therefore is time and depth dependent (typical flow rate 0.00045 d^{-1} in summer to 2.6 d^{-1} in winter). Mathematically, the imposed flow is identical to dilution in a chemostat, diffusion between the modeled compartment and an outside source, or relaxation toward a reference state. Effectively, the flow reintroduces extinct species, and thus provides the permanent background diversity proposed for SIDs. Given its coupling with diffusivity, it is best thought of as a parameterization of horizontal transport and diffusion in a horizontally heterogeneous environment; its effect on diversity is similar to assumptions of a minimal population density (Burchard et al. 2006) or a constant diversity (Wirtz and Eckhardt 1996).

Results

Figure 2 shows the light forcing and the response of biota and nutrient levels at the depth-averaged open ocean site. The light intensity (Fig. 2a) is visibly governed by a sinusoidal seasonal cycle on which noise due to rapid, erratic variation in cloud cover is imposed. Following the gradual increase in light intensity, a phytoplankton bloom develops in spring (Fig. 2b). In early summer most nutrient has been fixed in phytoplankton biomass. In the absence of

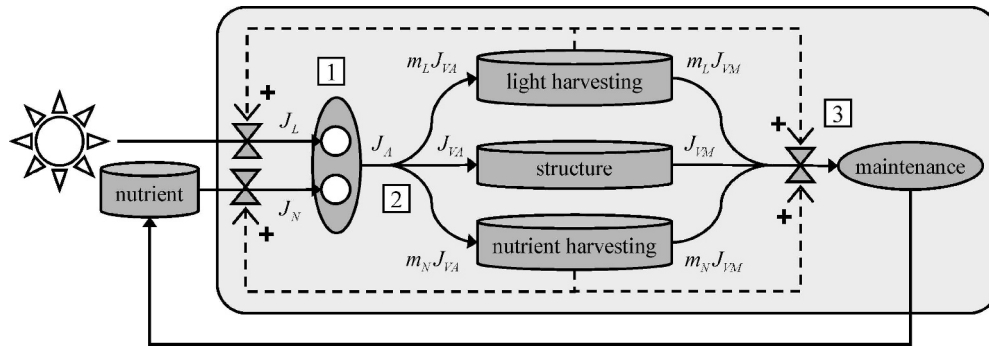


Fig. 1. Two-trait model of a phytoplankton population. Solid lines denote mass or energy fluxes or both, from left to right. (1) Light and nutrient are combined by the two-substrate synthesizing unit (ellipse, contained circles symbolize substrate binding sites) to produce new biomass. (2) Newly produced biomass is partitioned over the light-harvesting, nutrient-harvesting, and structure pools (can symbols) according to partition coefficients m_L and m_N . (3) The biomass pools are subject to turnover because of maintenance; biomass that is broken down returns to the environment as inorganic nutrient. Dashed lines signify (positive) feedbacks between harvesting biomass and metabolic rates at the location of the hourglass symbols: Harvesting biomasses enhance substrate availability (left), but also increase maintenance costs (right).

grazers, this low-nutrient, high-biomass situation persists all over summer, to be finally terminated in autumn by the gradual reduction in light intensity. Figure 2c,d shows the response of the phytoplankton community to changes in light and nutrient, visualized as the marginals (i.e., the individual distributions of light- and nutrient-harvesting investments), means, and 10th and 90th percentiles of the bivariate trait distribution over time. Foremost, one can observe that during the bloom, the typical light-harvesting investment (e.g., its mean or modus) decreases slightly,

whereas the nutrient-harvesting investment increases. As species-specific harvesting investments are fixed, this indicates a change in community structure. Second, one can observe that the highest community diversity—quantified by the distance between the percentiles—occurs in winter; during the development of the bloom diversity steadily decreases. Figure 3 shows the full bivariate trait distribution at the beginning (Fig. 3a) and at the peak of the bloom (Fig. 3b); again, the shift in investments and the decrease in diversity can be seen. We may note that

Table 1. Symbols used in the phytoplankton SID. Shown respectively, state and forcing variables (the latter supplied by the physical model), traits, parameters, reference concentrations used for initialization and immigration, and intermediate variables used in the model description only. Note that saturation coefficients K_L and K_N are references applicable when trait values m_L and m_N equal one, respectively; the effective half saturation coefficients equal K_L / m_L and K_N / m_N .

Symbol	Interpretation	Unit	Value
V	Structural biomass	$\mu\text{mol L}^{-1}$	
X_N	Nutrient	$\mu\text{mol L}^{-1}$	
X_L	Light intensity	W m^{-2}	
D	Turbulent diffusivity	$\text{m}^2 \text{d}^{-1}$	
m_L	Light-harvesting investment	—	
m_N	Nutrient-harvesting investment	—	
r_{max}	Maximum specific growth rate	d^{-1}	1.5
K_L	Reference light half-saturation coefficient	W m^{-2}	2
K_N	Reference nutrient half-saturation coefficient	$\mu\text{mol L}^{-1}$	0.25
k	Rate of biomass turnover	d^{-1}	0.05
κ	Immigration rate relative to turbulent diffusivity	m^{-2}	0.0001
$X_{N,\text{ref}}$	Reference nutrient concentration	$\mu\text{mol L}^{-1}$	4
$V_{i,\text{ref}}$	Reference structural biomass concentration for species i	$\mu\text{mol L}^{-1}$	0.0008
J_L	Light availability for biomass production	$\text{J L}^{-1} \text{d}^{-1}$	
J_N	Nutrient availability for biomass production	$\mu\text{mol L}^{-1} \text{d}^{-1}$	
y_L	Light needed per unit of produced biomass	$\text{J } \mu\text{mol}^{-1}$	
y_N	Nutrient needed per unit of produced biomass	—	
J_{Am}	Maximum rate of biomass production	$\mu\text{mol L}^{-1} \text{d}^{-1}$	
J_A	Rate of biomass production	$\mu\text{mol L}^{-1} \text{d}^{-1}$	
J_{VA}	Rate of structural biomass production	$\mu\text{mol L}^{-1} \text{d}^{-1}$	
J_{VM}	Structural biomass turnover due to maintenance	$\mu\text{mol L}^{-1} \text{d}^{-1}$	

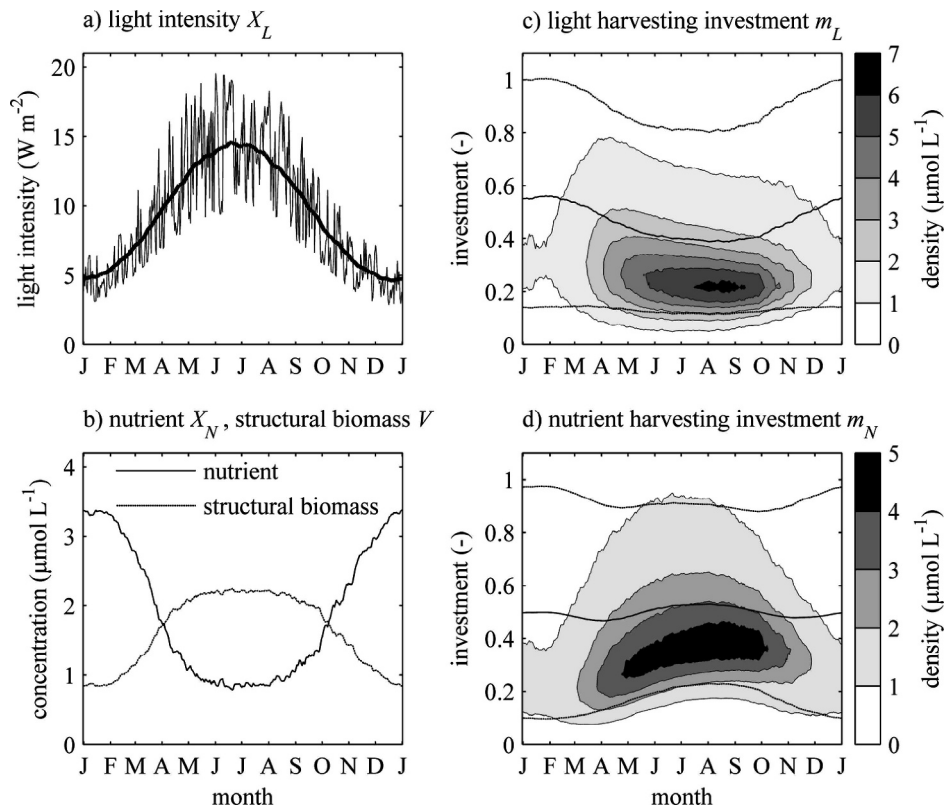


Fig. 2. Simulated light forcing (a), nutrient and structural biomass (b), light-harvesting investment (c), and nutrient-harvesting investment (d) at the depth-averaged open ocean site. The light intensity is shown as the daily averaged signal (thin line) and its 90-d running mean (thick line). Structural biomass is integrated over the whole trait distribution, i.e., it equals the lump sum of all virtual species. Harvesting investments are shown as the nonnormalized marginal densities of the bivariate trait distribution in time (gray scale), calculated by summing the discretized distribution (see also Fig. 3) over one trait dimension and dividing by the grid step of the other trait. In addition, it shows the means (solid line) and 10th and 90th percentiles (dashed lines) of the marginal densities.

Fig. 2c,d are related to Fig. 3: The former each shows a marginal of the latter bivariate distribution—i.e., that distribution integrated over one trait axis—in time.

Resolution of the vertical structure of the site introduces several new phenomena. Light attenuation with depth produces a vertical gradient of light availability (Fig. 4a), and a time- and depth-dependent mixing intensity (Fig. 4b) controls distribution of nutrient and biomass over depth, as well as the rate of immigration. Despite these differences, the trends in nutrient (Fig. 4c) and structural biomass (Fig. 4d) in the upper layers resemble those seen for the depth-averaged setup: A phytoplankton bloom starts in spring, shortly after which the surface is depleted of nutrient; in autumn the community collapses and nearly all biomass is remineralized. Only beyond 100-m depth a different trend is seen. There, lack of light limits phytoplankton growth throughout the year and nutrient levels remain high. Similarly, the phytoplankton community structure in surface waters behaves qualitatively as in the depth-averaged setup. The mean nutrient-harvesting investment increases while the bloom persists, at the expense of the mean light-harvesting investment (Fig. 4e,f).

In deeper water (>65 m), however, the mean light-harvesting investment increases sharply at the onset of the bloom and remains relatively high throughout its life span, whereas the mean nutrient-harvesting investment initially decreases to minimum levels and remains low. This switch between the nutrient- and light-harvesting regimes occurs around 65 m, and could therefore not be reproduced with the depth-averaged setup, which described the top 150 m. Because of resolution of these two distinct regimes, the spatially explicit setup also permits more extreme trait value means: effective ranges of mean light-harvesting investments (0.17–0.62, Fig. 4e) and nutrient-harvesting investments (0.25–0.63, Fig. 4f) are substantially larger than with the depth-averaged setup (respectively 0.39–0.56 and 0.47–0.53, Figs. 2c,d).

Discussion

Phytoplankton community structure—The behavior of the phytoplankton community can be viewed as a direct result of a time- and depth-varying environmental selection

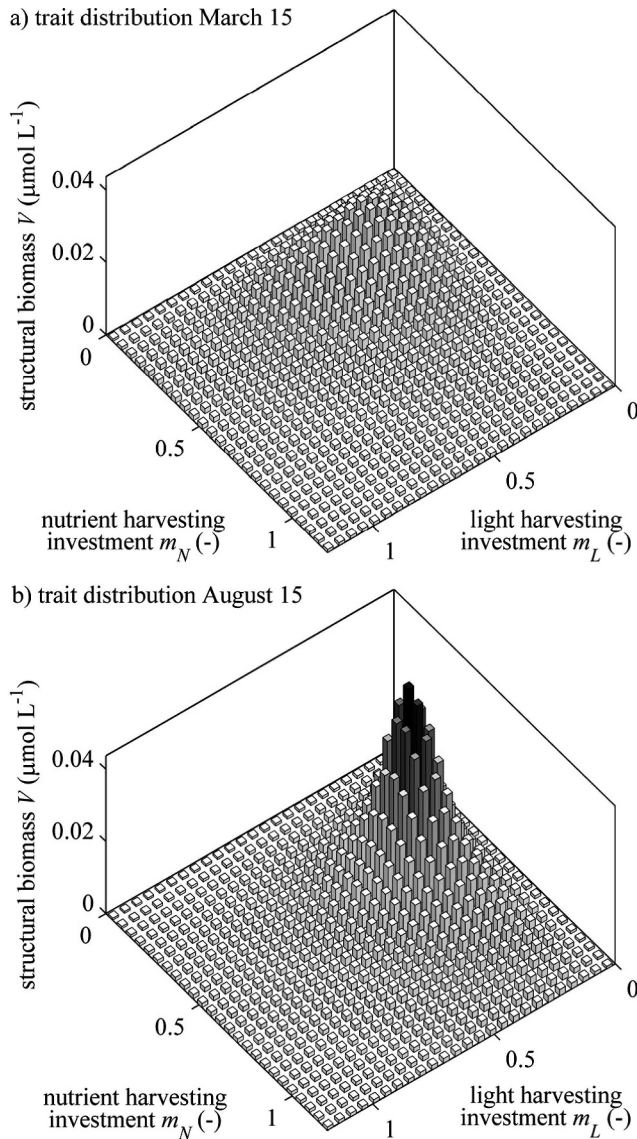


Fig. 3. The discretized trait distribution at the start (a) and peak (b) of the bloom, at the depth-averaged open ocean site. Every bar represents a simulated virtual phytoplankton species; the height of the bar denotes the amount of structural biomass in that species.

pressure. During the first few months phytoplankton experience low light levels, due to low solar radiation as well as strong mixing (the latter in the vertically structured setup only). In this period light limits phytoplankton growth to such extent that biota levels are nearly negligible and the nutrient concentration remains high. The few individuals that do persist are selected for light affinity rather than nutrient affinity; consequently, the column at the onset of the bloom is dominated by species with high investment in light harvesting (high m_L) and low investment in nutrient harvesting (low m_N). Shortly after the onset of the bloom, nutrient is depleted near the surface while light is amply available. This new situation favors species with high nutrient affinity, which can be seen to become more

abundant as depletion persists. A different trend is seen in deeper waters (>65 m) in the vertically structured setup. There, nutrient is more readily available as it diffuses upward from nutrient-rich deep waters, whereas light intensity has dropped to such an extent that it limits growth. This dark environment favors investment in light harvesting over nutrient harvesting, causing species with a high investment in light harvesting (high m_L) to become more abundant. Species with high light affinity—out-competed by nutrient-harvesting species near the surface after the initial bloom phase—thus manage to find a niche in deeper water layers. This summer situation is reminiscent of the classic two-layer model with nutrient-limited dynamics near the surface and light-limited dynamics near the deep (Dugdale 1967).

The product of the mean harvesting investment (Fig. 4e,f) and the structural biomass (Fig. 4d) describes the biomass allocated to resource harvesting, shown for light harvesting in Fig. 5. Light-harvesting biomass is high at the onset of the bloom, and in deeper waters (85 m, where 1.4% of the surface radiation remains) afterward. It is common practice to assume that light-harvesting biomass consists in part of chlorophyll (Geider et al. 1996; Klausmeier et al. 2004). Under this assumption the model predicts formation of a maximum chlorophyll concentration near the base of the euphotic zone, which persists independent of any maximum in total biomass (which here—with neutrally buoyant biota—is simply highest near the surface; Fig. 4d). This subsurface chlorophyll maximum is a well-known, ubiquitous feature of aquatic ecosystems (Fennel and Boss 2003). Its persistence independent of (structural) biomass has to our knowledge exclusively been demonstrated in models that accommodate photoacclimation, i.e., regulation of chlorophyll contents on the physiological level (Fennel and Boss 2003); this applies for instance to the models of Geider et al. (1996, 1998). The present biodiversity-inspired model demonstrates an alternative: A subsurface chlorophyll maximum can arise through species-sorting processes that favor high-chlorophyll “shade” species in the high-nutrient, low-light deep, as opposed to low-chlorophyll species with high nutrient affinity near the surface. This matches the concept of a “shade flora,” i.e., the idea that some species are preferentially located in deep levels of the euphotic zone, which was put forward already at the end of the 19th century (Sournia 1982b). Variation in species assemblages with depth has been found at numerous locations including the simulated site (Bidigare et al. 1990; Kemp et al. 2000). Although the depth-specific assemblages of phytoplankton species are known to show great taxonomic variety (Sournia 1982b; Venrick 1982), they are commonly thought to show homogeneity in physiological features; early studies already suggested a link between preferential depth of species and their light affinity (Ryther 1956). It has been demonstrated that some deep-dwelling species are indeed capable of growing under very-low-light conditions (Goldman 1993), indicating that these species indeed possess a higher light affinity. If we assume that light affinity correlates with chlorophyll content, these observations indicate that the subsurface chlorophyll maximum may

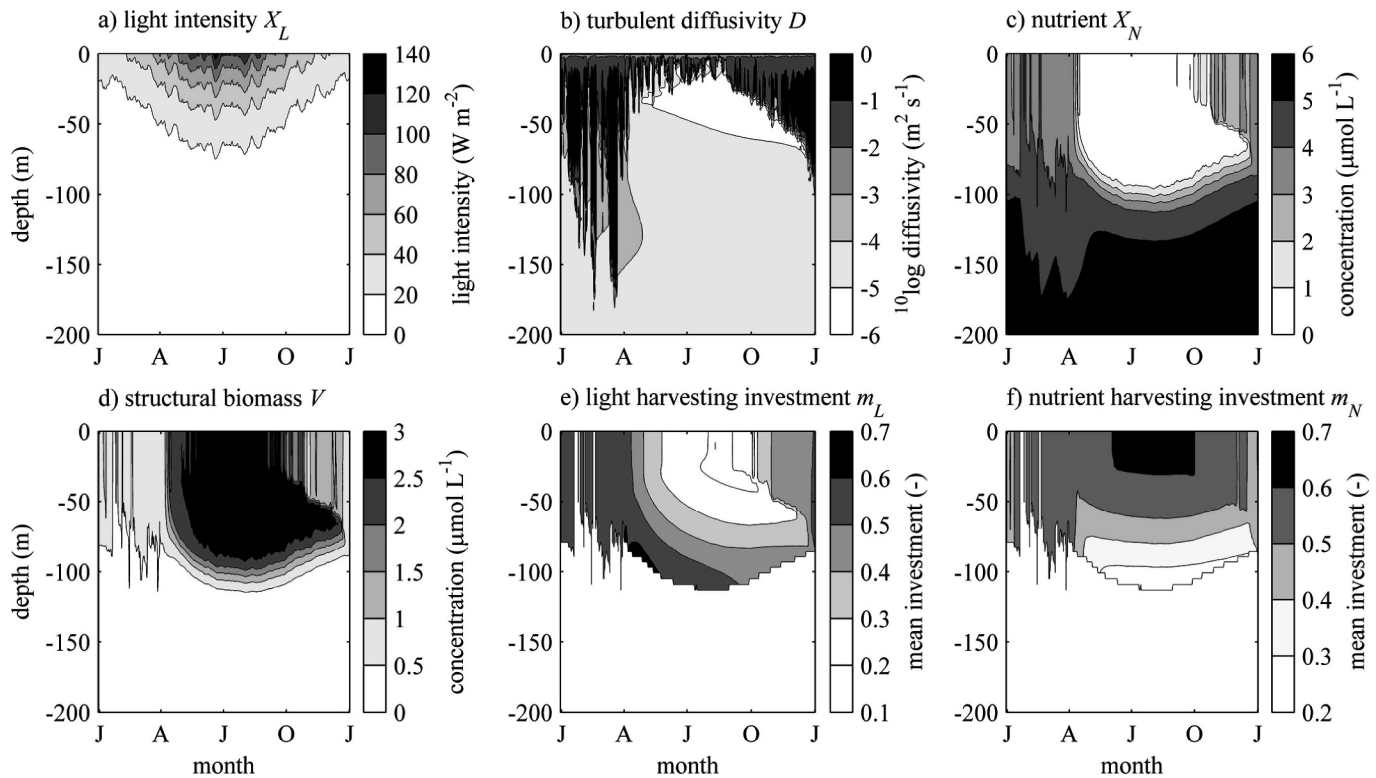


Fig. 4. Simulated forcing, nutrient, biomass, and trait means as a function of time (horizontal) and depth (vertical) for the vertically structured setup. Shown respectively, daily mean of the light intensity (a), turbulent diffusivity (b), nutrient concentration (c), structural biomass concentration (d), the mean light-harvesting investment (e), and the mean nutrient-harvesting investment (f). Structural biomass is integrated over the whole trait distribution, i.e., it represents the lump sum of all virtual species. Mean investments are masked where the total structural biomass does not exceed the immigrating background level of $0.5 \mu\text{mol L}^{-1}$; this is the case in deep water, typically below 100 m. Gray scales correspond to the value of the plotted variables, with white denoting complete absence, as indicated by the scale on the right. Only the top 200 m of the water column is shown; beyond this level, plotted variables do not change with increasing depth.

indeed at least in part arise through local concentration of species with high light affinity and chlorophyll content, as suggested by our results.

In Margalef's Mandala (Margalef 1978), phytoplankton succession is viewed as traversing a phase plane defined by nutrient concentration on the one hand and turbulence on the other. The initial high-turbulence, high-nutrient environment is replaced by a stratified depleted environment as the year progresses, with distinct niches for different groups of species (respectively: diatoms, coccolithophorids, dinoflagellates) along this trajectory. Margalef explained this succession in terms of differential species-specific affinities for limiting nutrients, which in turn have been linked to morphology and cell size (Sournia 1982a; Aksnes and Egge 1991; Chisholm 1992). The concept of affinity-driven succession applies seamlessly to (near-surface) seasonal succession as observable in our results: As the bloom persists, colonizing species with low nutrient affinities are replaced by species with higher nutrient affinity. Thus, our result corroborates that nutrient availability and differences in nutrient affinity may control succession; this is also tentatively indicated by in-situ microcosm experiments demonstrating that nitrate addition in oligotrophic environments greatly changes the phytoplankton community structure (Carter et al. 2005).

Several studies have suggested that the capacities for light and nutrient harvesting in phytoplankton might be negatively correlated (Huisman and Weissing 1995; Leibold 1997). In the present model such a correlation is not

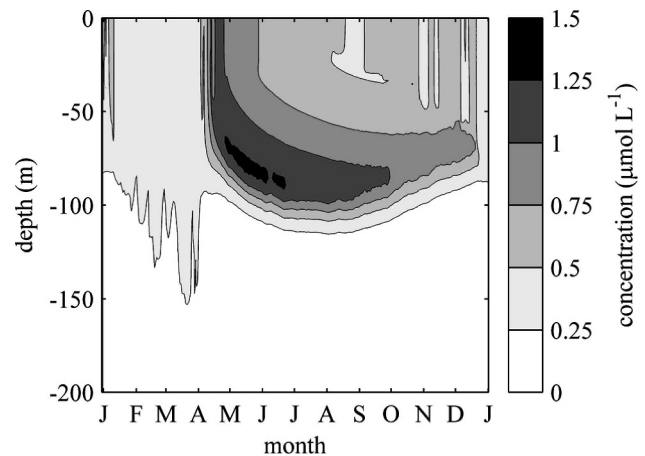


Fig. 5. Light-harvesting biomass as a function of time (horizontal) and depth (vertical) for the vertically structured setup. This quantity equals the product of structural biomass (Fig. 4d) and the mean light-harvesting investment (Fig. 4e), and can serve as chlorophyll proxy.

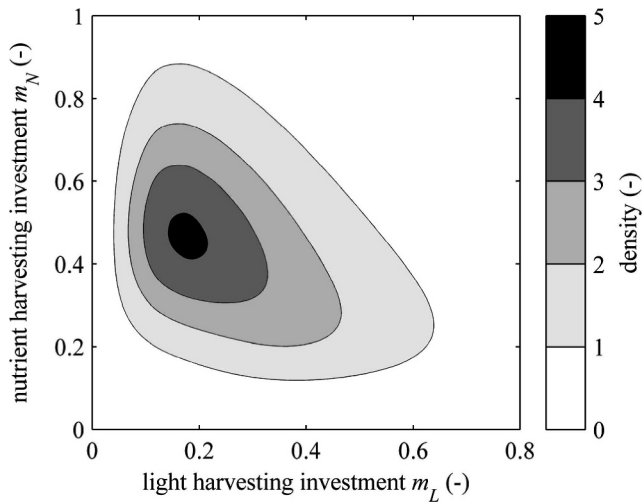


Fig. 6. Depth- and time-integrated species abundance as function of light- and nutrient-harvesting investment. The distribution is normalized so its integral equals one, and can consequently be interpreted as a probability distribution of combinations of harvesting investments. Note that harvesting investments m_L and m_N are inversely proportional to the effective half-saturation coefficients, which equal K_L / m_L and K_N / m_N , respectively.

imposed. The individual capacities for light and nutrient harvesting are each independently governed by a harvest-growth trade-off, but the model does not incorporate an explicit negative feedback between light and nutrient harvesting. Yet in Fig. 4e,f a negative correlation between the two harvesting investments emerges. The environment appears to advocate either investment in light harvesting (in the dark) or investment in nutrient harvesting (in periods of depletion), but not both. Figure 6 illustrates that a slight negative correlation (-0.05) persists when integrating the trait distribution over time and space. As a result, random sampling of phytoplankton species could indicate a trade-off between light and nutrient affinity. However, the indirect light-nutrient trade-off that emerges from our results is therefore not nearly as strong (in terms of correlation) as other phytoplankton trade-offs that have been suggested to govern phytoplankton strategies (Wirtz and Eckhardt 1996; Huisman and Weissing 2001). If the mechanisms underlying our trade-off are real, its subtlety could explain why the existence of a trade-off between light and nutrient harvesting has as yet not been convincingly demonstrated (Huisman and Weissing 2001; Passarge et al. 2006).

Not all differences in competitive ability between phytoplankton species relate to differences in light and nutrient affinity. Some studies have argued against a determining role of nutrient affinity in seasonal succession (Smayda 1997; Smayda and Reynolds 2001), pointing out that nutrient affinity often is a poor predictor of the order of species appearance. For instance, diatoms commonly dominate the first, nutrient-rich stages of the spring bloom, but are known to possess high nutrient affinities. Smayda (1997) presented four alternative determinants of species

appearance in the successional sequence: (1) nutrient retrieval mechanisms, (2) mixotrophic nutritional tendency, (3) allelochemically enhanced interspecific competition, and (4) allelopathic antipredation defense mechanisms. Of these mechanisms, the first can be accounted for in the present model. Nutrient-harvesting biomass comprises all mass that directly or indirectly contributes to nutrient retrieval, and could therefore include structures that allow local motility, causing cells to shed stagnant water mantles that limit diffusion-mediated nutrient arrival. However, the other three mechanisms cannot directly be linked to nutrient-harvesting biomass, and would therefore require qualitatively different models. Additionally, the current approach neglects direct selection by predators. If losses due to predation are substantial, differences in phytoplankton fitness might better relate to the species' susceptibility to predators than to differences in affinity (Carpenter and Kitchell 1996). The present study focuses primarily on succession in oligotrophic open ocean sites, where predation often plays only a minor role (Steinberg et al. 2001); extension of the approach to aquatic environments where mortality due to predation is high could necessitate the introduction of defense or edibility traits (Wirtz and Eckhardt 1996). Although beyond the scope of this study, we intend to investigate the role of other phytoplankton traits in the future. In particular, mixotrophy is a suitable test case as it can be incorporated in SID-type models through allocation rules (distinguishing autotrophic and heterotrophic harvesting biomass), and would simultaneously allow the SID approach to span more functional groups (e.g., heterotrophic bacteria) (Troost et al. 2005); preliminary results indicate that differences in mixotrophic tendency can explain shifts in species composition and the ratio algae : bacteria in time and depth (in preparation).

Biodiversity—Changes in community structure are the result of selection pressure applied to assemblages of different species (Levin 1998; Leibold and Norberg 2004). The amount of diversity controls the rate at which the community responds to selection pressure (Wirtz and Eckhardt 1996; Norberg et al. 2001); diversity thus plays a major role in SID-type models that describe the adaptive behavior of communities. The presence and persistence of biodiversity is often linked to spatiotemporal heterogeneity (Tilman et al. 1982; Tilman and Kareiva 1997; Chesson 2000). In the present study, temporal heterogeneity is established through a noisy seasonally fluctuating light intensity, which proves capable of inducing seasonal changes in community structure, independent of the presence of an explicit spatial structure (Fig. 2c,d). However, the time-varying light intensity cannot sustain diversity. Similar to other studies (Norberg et al. 2001), most diversity is lost within a year if we do not impose continuous species immigration (not shown). For the vertically explicit setup, one might expect spatial heterogeneity to sustain biodiversity. However, we find that the vertical light gradient combined with diffusion-mediated dispersal is insufficient for maintenance of a realistic biodiversity. In the absence of immigration from outside sources most diversity is again lost over time, though,

similar to other studies (Troost et al. 2005), a low number of species appears able to coexist. Not surprisingly, the rate of immigration is a key parameter in both setups. A weak input cannot sustain substantial variance and causes the system to lose adaptive ability, whereas a strong input keeps the community close to its reference state and prevents it from adapting. In this respect, immigration as implemented in the vertically structured setup arguably strikes an ideal balance. With immigration proportional to the turbulent mixing intensity, it nearly subsides in summer, allowing for significant specialization (i.e., changes in the mean trait value, Fig. 4e,f), while in winter it greatly increases and resets the system to a state of high diversity. Consequently the system at times displays strong specialization without permanently surrendering a realistic level of diversity.

Systems of infinite diversity—A SID acquires rich dynamics through incorporation of competition and succession, and as such can display a wealth of realistic behaviors despite a lack of physiological detail and parameters. However, in their present form SIDs require considerable computational effort. Discretization of the trait distribution requires many state variables to represent the different (virtual) species, which makes simulation expensive. This would discard the SID approach for many practical purposes, in particular for application in detailed spatially explicit models such as general circulation models. This problem can be avoided by abandoning discretization of trait distributions. Recent studies have shown that trait distributions are often well captured by the first distributional moments, i.e., mean, variance, skewness, and kurtosis (Wirtz and Eckhardt 1996; Norberg et al. 2001). Rather than discretizing the distribution, one may obtain an accurate approximation of its dynamics by modeling the dynamics of the first few moments. Wirtz and Eckhardt (1996) proposed the effective variable approach, which assumes the trait distribution can be approximated by a normal distribution; they subsequently take its variance constant and evolve the mean. Similarly, Norberg et al. (2001) evolve the mean and variance of an arbitrary univariate trait distribution using simulation-based parameterizations of its skewness and kurtosis. For the present phytoplankton SID, we have obtained good results by assuming a (bivariate) lognormal trait distribution and evolving its mean and covariances. Depth- and time-averaged deviations from the present results equaled 1.2% for structural biomass, 6.6% for the mean, and 10.3% for the covariances, measured relative to the respective maximum ranges (in preparation). Although reduction of the trait distribution to the first few moments can in theory eliminate interesting dynamics (in particular multimodality), we deem it a promising direction for further expansion of the SID concept. Given that the number of state variables necessary for discretized trait distributions increases exponentially with the number of traits, it will certainly prove indispensable for modeling systems with more than two traits.

The phytoplankton SID integrates separate theories dealing with species diversity and succession. It demon-

strates changes in species composition with depth as proposed by the concept of a shade flora, as well as seasonal succession in time, in line with Margalef (1978). It does so with a minimum of parameters (four), and as such might be said to successfully illustrate the potential of biodiversity-based approaches to aquatic ecosystem modeling. Obviously, the present model lacks a wealth of physiological detail (Geider et al. 1998; Flynn 2001; Pahlow 2005), and will not reproduce some features that emerge from detailed laboratory studies (e.g., photoinhibition, nutrient buffering). However, for understanding of aquatic ecosystems as a whole, we believe models will benefit more from improved representations of biodiversity and succession than from more accurate representations of (partially species-specific) physiological processes. The SID approach could be a starting point for a next generation of ecosystem models.

References

- ABRAMS, P. A., H. MATSUDA, AND Y. HARADA. 1993. Evolutionarily unstable fitness maxima and stable fitness minima of continuous traits. *Evol. Ecol.* **7**: 465–487.
- AKSNES, D. L., AND J. K. EGGE. 1991. A theoretical model for nutrient uptake in phytoplankton. *Mar. Ecol. Prog. Ser.* **70**: 65–72.
- ANDERSON, D. M., AND K. RENGFORNS. 2006. Community assembly and seasonal succession of marine dinoflagellates in a temperate estuary: The importance of life cycle events. *Limnol. Oceanogr.* **51**: 860–873.
- ANDERSON, T. R. 2005. Plankton functional type modelling: Running before we can walk? *J. Plankton Res.* **27**: 1073–1081.
- BAAS-BECKING, L. G. M. 1934. *Geobiologie of inleiding tot de milieukunde*. W. P. van Stockum & Zoon N.V.
- BARETTA, J. W., W. EBENHÖH, AND P. RUARDIJ. 1995. The European regional seas ecosystem model, a complex marine ecosystem model. *Neth. J. Sea Res.* **33**: 233–246.
- BEIJERINCK, M. W. 1913. *De infusies en de ontdekking der bacteriën*. Jaarboek van de Koninklijke Akademie v. Wetenschappen. Müller.
- BIDIGARE, R. R., J. MARRA, T. D. DICKEY, R. ITURRIAGA, K. S. BAKER, R. C. SMITH, AND H. PAK. 1990. Evidence for phytoplankton succession and chromatic adaptation in the Sargasso Sea during spring 1985. *Mar. Ecol. Prog. Ser.* **60**: 113–122.
- BURCHARD, H., K. BOLDING, W. KUHN, A. MEISTER, T. NEUMANN, AND L. UMLAUF. 2006. Description of a flexible and extendable physical-biogeochemical model system for the water column. *J. Mar. Syst.* **61**: 180–211.
- , ———, AND M. RUIZ VILLARREAL. 1999. GOTM—a general ocean turbulence model. Theory, applications and test cases European Commission.
- CARPENTER, S. R. AND J. F. KITCHELL [EDS.]. 1996. *The trophic cascade in lakes*. Cambridge Univ. Press.
- CARTER, C. M., A. H. ROSS, D. R. SCHIEL, C. HOWARD-WILLIAMS, AND B. HAYDEN. 2005. In situ microcosm experiments on the influence of nitrate and light on phytoplankton community composition. *J. Exp. Mar. Biol. Ecol.* **326**: 1–13.
- CHESSON, P. 2000. Mechanisms of maintenance of species diversity. *Ann. Rev. Ecol. Syst.* **31**: 343–366.
- CHISHOLM, S. 1992. Phytoplankton size. In P. Falkowski and A. D. Woodhead [eds.], *Primary production and biogeochemical cycles in the sea*. Plenum Press.

- CLOERN, J. E., AND R. DUFFORD. 2005. Phytoplankton community ecology: Principles applied in San Francisco Bay. *Mar. Ecol. Prog. Ser.* **285**: 11–28.
- DIECKMANN, U., AND R. LAW. 1996. The dynamical theory of coevolution: A derivation from stochastic ecological processes. *J. Math. Biol.* **34**: 579–612.
- DIEHL, S. 2002. Phytoplankton, light, and nutrients in a gradient of mixing depths: Theory. *Ecology* **83**: 386–398.
- DUGDALE, R. C. 1967. Nutrient limitation in sea—dynamics identification and significance. *Limnol. Oceanogr.* **12**: 685–695.
- EBENHÖH, W., J. G. BARETTA-BEKKER, AND J. W. BARETTA. 1997. The primary production module in the marine ecosystem model ERSEM II, with emphasis on the light forcing. *J. Sea Res.* **38**: 173–193.
- FENNEL, K., AND E. BOSS. 2003. Subsurface maxima of phytoplankton and chlorophyll: Steady-state solutions from a simple model. *Limnol. Oceanogr.* **48**: 1521–1534.
- FLYNN, K. J. 2001. A mechanistic model for describing dynamic multi-nutrient, light, temperature interactions in phytoplankton. *J. Plankton Res.* **23**: 977–997.
- GEIDER, R. J., H. L. MACINTYRE, AND T. M. KANA. 1996. A dynamic model of photoadaptation in phytoplankton. *Limnol. Oceanogr.* **41**: 1–15.
- , ———, AND T. M. KANA. 1998. A dynamic regulatory model of phytoplanktonic acclimation to light, nutrients, and temperature. *Limnol. Oceanogr.* **43**: 679–694.
- GOLDMAN, J. C. 1993. Potential role of large oceanic diatoms in new primary production. *Deep-Sea Res. I.* **40**: 159–168.
- HANSKI, I. 1999. *Metapopulation ecology*. Oxford Univ. Press.
- HUISMAN, J., AND F. J. WEISSING. 1995. Competition for nutrients and light in a mixed water column—a theoretical analysis. *Am. Nat.* **146**: 536–564.
- , AND ———. 2001. Biological conditions for oscillations and chaos generated by multispecies competition. *Ecology* **82**: 2682–2695.
- JIANG, L., O. M. E. SCHOFIELD, AND P. G. FALKOWSKI. 2005. Adaptive evolution of phytoplankton cell size. *Am. Nat.* **166**: 496–505.
- KEMP, A. E. S., J. PIKE, R. B. PEARCE, AND C. B. LANGE. 2000. The “fall dump”—a new perspective on the role of a “shade flora” in the annual cycle of diatom production and export flux. *Deep-Sea Res. II.* **47**: 2129–2154.
- KLAUSMEIER, C. A., E. LITCHMAN, T. DAUFRESNE, AND S. A. LEVIN. 2004. Optimal nitrogen-to-phosphorus stoichiometry of phytoplankton. *Nature* **429**: 171–174.
- KOOIJMAN, S. A. L. M. 1998. The synthesizing unit as model for the stoichiometric fusion and branching of metabolic fluxes. *Biophys. Chem.* **73**: 179–188.
- . 2000. *Dynamic energy and mass budgets in biological systems*, 2nd rev. ed. Cambridge Univ. Press.
- , H. A. DIJKSTRA, AND B. W. KOOI. 2002. Light-induced mass turnover in a mono-species community of mixotrophs. *J. Theor. Biol.* **214**: 233–254.
- KUIJPER, L. D. J., T. R. ANDERSON, AND S. A. L. M. KOOIJMAN. 2004. C and N gross growth efficiencies of copepod egg production studied using a Dynamic Energy Budget model. *J. Plankton Res.* **26**: 213–226.
- LANCELOT, C., AND OTHERS. 2005. Modelling diatom and Phaeocystis blooms and nutrient cycles in the Southern Bight of the North Sea: The MIRO model. *Mar. Ecol. Prog. Ser.* **289**: 63–78.
- LEIBOLD, M. A. 1997. Do nutrient-competition models predict nutrient availabilities in limnetic ecosystems? *Oecologia* **110**: 132–142.
- , AND J. NORBERG. 2004. Biodiversity in metacommunities: Plankton as complex adaptive systems? *Limnol. Oceanogr.* **49**: 1278–1289.
- LEVIN, S. A. 1998. Ecosystems and the biosphere as complex adaptive systems. *Ecosystems* **1**: 431–436.
- MARGALEF, R. 1978. Life-forms of phytoplankton as survival alternatives in an unstable environment. *Oceanol. Acta* **1**: 493–509.
- MERICO, A., T. TYRRELL, E. J. LESSARD, T. OGUZ, P. J. STABENO, S. I. ZEEMAN, AND T. E. WHITLEDGE. 2004. Modelling phytoplankton succession on the Bering Sea shelf: Role of climate influences and trophic interactions in generating *Emiliania huxleyi* blooms 1997–2000. *Deep-Sea Res. I.* **51**: 1803–1826.
- MUNK, W. H., AND G. A. RILEY. 1952. Absorption of nutrients by aquatic plants. *J. Mar. Res.* **11**: 215–240.
- NORBERG, J. 2004. Biodiversity and ecosystem functioning: A complex adaptive systems approach. *Limnol. Oceanogr.* **49**: 1269–1277.
- , D. P. SWANEY, J. DUSHOFF, J. LIN, R. CASAGRANDE, AND S. A. LEVIN. 2001. Phenotypic diversity and ecosystem functioning in changing environments: A theoretical framework. *Proc. Natl. Acad. Sci. USA* **98**: 11376–11381.
- PAHLOW, M. 2005. Linking chlorophyll–nutrient dynamics to the Redfield N:C ratio with a model of optimal phytoplankton growth. *Mar. Ecol. Prog. Ser.* **287**: 33–43.
- PASSARGE, J., S. HOL, M. ESCHER, AND J. HUISMAN. 2006. Competition for nutrients and light: Stable coexistence, alternative stable states, or competitive exclusion? *Ecol. Monogr.* **76**: 57–72.
- POLIS, G. A., W. B. ANDERSON, AND R. D. HOLT. 1997. Toward an integration of landscape and food web ecology: The dynamics of spatially subsidized food webs. *Ann. Rev. Ecol. Syst.* **28**: 289–316.
- QUÉRÉ, C. L., AND OTHERS. 2005. Ecosystem dynamics based on plankton functional types for global ocean biogeochemistry models. *Glob. Change Biol.* **11**: 2016–2040.
- RAICK, C., K. SOETAERT, AND M. GREGOIRE. 2006. Model complexity and performance: How far can we simplify? *Prog. Oceanogr.* **70**: 27–57.
- RYTHER, J. H. 1956. Photosynthesis in the ocean as a function of light intensity. *Limnol. Oceanogr.* **1**: 61–70.
- SHUTER, B. 1979. Model of physiological adaptation in unicellular algae. *J. Theor. Biol.* **78**: 519–552.
- SMAYDA, T. J. 1997. Harmful algal blooms: Their ecophysiology and general relevance to phytoplankton blooms in the sea. *Limnol. Oceanogr.* **42**: 1137–1153.
- , AND C. S. REYNOLDS. 2001. Community assembly in marine phytoplankton: Application of recent models to harmful dinoflagellate blooms. *J. Plankton Res.* **23**: 447–461.
- SOMMER, U. 1985. Comparison between steady-state and non-steady state competition—experiments with natural phytoplankton. *Limnol. Oceanogr.* **30**: 335–346.
- SOURNIA, A. 1982a. Form and function in marine phytoplankton. *Biol. Rev. Camb. Philos. Soc.* **57**: 347–394.
- . 1982b. Is there a shade flora in the marine plankton. *J. Plankton Res.* **4**: 391–399.
- STEINBERG, D. K., C. A. CARLSON, N. R. BATES, R. J. JOHNSON, A. F. MICHAELS, AND A. H. KNAP. 2001. Overview of the US JGOFS Bermuda Atlantic Time-series Study (BATS): A decade-scale look at ocean biology and biogeochemistry. *Deep-Sea Res. II.* **48**: 1405–1447.
- TILMAN, D. 1982. *Resource competition and community structure*. Princeton Univ. Press.
- , AND P. M. KAREIVA. 1997. *Spatial ecology: The role of space in population dynamics and interspecific interactions*. Princeton Univ. Press.

- , S. S. KILHAM, AND P. KILHAM. 1982. Phytoplankton community ecology—the role of limiting nutrients. *Ann. Rev. Ecol. Syst.* **13**: 349–372.
- TROOST, T. A., B. W. KOOL, AND S. A. L. M. KOOIJMAN. 2005. Ecological specialization of mixotrophic plankton in a mixed water column. *Am. Nat.* **166**: E45–E61.
- VENRICK, E. L. 1982. Phytoplankton in an oligotrophic ocean—observations and questions. *Ecol. Monogr.* **52**: 129–154.
- WIRTZ, K. W., AND B. ECKHARDT. 1996. Effective variables in ecosystem models with an application to phytoplankton succession. *Ecol. Mod.* **92**: 33–53.

Received: 18 May 2006
Accepted: 27 January 2007
Amended: 11 March 2007